GEOPHYSICAL RESEARCH LETTERS, VOL. 27, NO. 18, PAGES 2885-2888, SEPTEMBER 15, 2000

Source Regions of the Slow Solar Wind in Coronal Streamers

L. Ofman

Raytheon ITSS and NASA Goddard Space Flight Center, Greenbelt, Maryland

Abstract. Recent SOHO/UVCS observations of the O^{5+} ion line emission at 1032Å in coronal streamers indicate that the emission is stronger by an order of magnitude at the edges (legs) of streamers than in the central core of streamers. In contrast, the brightness of the Ly-α emission peaks in the core of streamers. I have developed the first 2.5D, three-fluid numerical MHD model of the slow solar wind flow in a coronal streamer. Using the model I find that the enhancement of the oxygen line emission occurs due to the enhanced abundances of O^{5+} ions in the legs of streamer caused by the Coulomb friction with the outflowing protons. Thus, the enhanced O^{5+} emission traces the source regions of the slow solar wind in coronal streamers. The identification of these regions helps to understand the origins and the composition of the slow solar wind.

Introduction

Recent Solar and Heliospheric (SOHO) Ultraviolet Coronagraph Spectrometer (UVCS) observations show that the physical properties of the minor ions in the corona provide clues on the coronal heating and solar wind acceleration mechanism. UVCS observations indicate that O^{5+} ions and other minor ions exceed temperatures of 10^7 K in coronal holes, and in streamers [*Kohl et al.*, 1997]. The UVCS observations show a striking difference in the appearance of coronal streamers in minor ion emission lines compared to hydrogen UV emission. These observations show that the emission from O^{5+} ions is stronger by an order of magnitude at the legs of streamers than in the central core of streamers (Figure 1). However, the brightness of the Ly-α emission peaks in the central core of streamers [*Kohl et al.*, 1997; *Raymond et al.*, 1997a].

Several possibilities which can explain the observed difference in the O^{5+} emission and Ly-α in streamers are discussed by *Noci et al.* [1997]. One of *Noci et al.* [1997] suggestions is that variation of minor ion abundance (i.e., ion density relative to proton density) may occur due to Coulomb friction with outflowing protons [*Geiss, Hirt, and Entwyler*, 1970] in a double-streamer geometry. *Noci et al.* concludes that only an abundance variation of O^{5+} across the streamer is consistent with the observations of other minor ion emissions in streamers, such as Mg^{9+} (625Å), Si^{6+} (499Å), and and Fe^{11+} (1242Å). *Raymond et al.* [1997a,b] suggested that gravitational settling in the core of streamers is the dominant mechanism for the depletion of O^{5+} there. However, the 1D single-fluid time-dependent model of the settling and diffusion of ions in the streamer core predicts that the abundance in the streamer legs is less than in the core of the streamer, in conflict with observations [*Raymond et al.*, 1997b].

Early computational models of O^{5+} ions in the solar wind did not include the full ion dynamics and treated the O^{5+} ions as test particles in one-dimensional solar wind flow [*Geiss, Hirt, and Entwyler*, 1970; *Joselyn and Holzer*, 1978; *Bürgi and Geiss*, 1986; *Esser and Leer*, 1990]. More recent multi-fluid studies of the flow of O^{5+} ions in the solar wind were confined to one spatial dimension [*Li, Esser, and Habbal*, 1997; *Raymond et al.*, 1997b]. Although these models made important contribution to our understanding of the minor-ion dynamics in the solar wind, the effects of coronal magnetic and density structure due to streamers were not included self-consistently.

Model Equations

To investigate the formation of the observed O^{5+} streamer I model the acceleration of the solar wind in a streamer by solving the three-fluid MHD equations with full ion dynamics [*Braginskii*, 1965] in spherical geometry. The 2.5D equations are obtained by taking $\partial/\partial\phi = 0$ in the 3D three-fluid MHD equations, i.e., by assuming azimuthal symmetry, and keeping all three components of the species velocities and fields. This simplification means that I model a streamer belt rather than an isolated streamer structure.

In the model I neglect electron inertia (since $m_e \ll m_p$, where m_e is the electron mass and m_p is the ion mass), relativistic effects ($V \ll c$), and assume quasi-neutrality of the plasma ($n_e = n_p + Zn_i$, where n_e is the electron density, n_p is the proton density, n_i is the ion density, and Z is the charge state of the ions). I neglect the ion-cyclotron terms since the relevant time scales are orders of magnitude larger the the ion gyro-period.

The normalized 3-fluid MHD equations are

$$\frac{\partial n_k}{\partial t} + \nabla\cdot(n_k\mathbf{V}_k) = 0, \quad (1)$$

$$n_k\left[\frac{\partial \mathbf{V}_k}{\partial t} + (\mathbf{V}_k\cdot\nabla)\mathbf{V}_k\right] = -E_k\nabla p_k - E_e\frac{Z_k n_k}{A_k n_e}\nabla p_e - \frac{n_k}{F_r r^2} + Z_k a_k\frac{n_k}{n_e}(\nabla\times\mathbf{B})\times\mathbf{B} + \mathbf{F}_{k,coul}, \quad (2)$$

$$\frac{\partial \mathbf{B}}{\partial t} = -\nabla\times\mathbf{E}, \quad \mathbf{E} = -\mathbf{V}_e\times\mathbf{B} + \frac{1}{S}\nabla\times\mathbf{B} \quad (3)$$

$$\mathbf{V}_e = \frac{1}{n_e}(n_p\mathbf{V}_p + Zn_i\mathbf{V}_i - b\nabla\times\mathbf{B}), \quad (4)$$

$$\frac{\partial T_k}{\partial t} = -(\gamma_k - 1)T_k\nabla\cdot\mathbf{V}_k - \mathbf{V}_k\cdot\nabla T_k, \quad (5)$$

where the index $k = p,\ i$, (in Equation (5) $k = e, p,\ i$), and p is protons, i is ions, and e is electrons. In the present model I assume that the corona is nearly isothermal (i.e., $\gamma_k \approx 1$), do not include heat sources explicitly, and neglect the thermal forces in the momentum equations. The viscous forces assumed to be negligible. I also neglected a temperature equilibration term in the energy equation due to heat

Paper number 2000GL000097.
0094-8276/00/2000GL000097$05.00

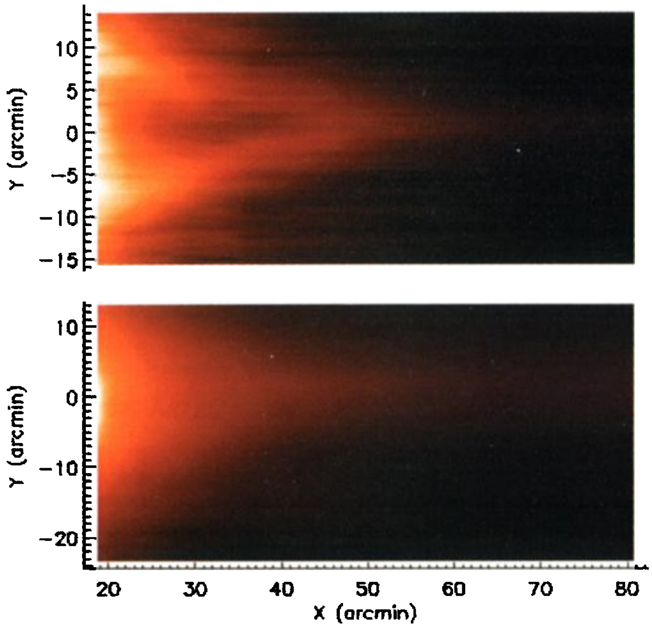

Figure 1. Images of the UVCS 12 October 1996 observation of an equatorial streamer above the west limb in O^{5+} (top panel) and in Lyman-α (bottom panel) EUV emissions. The spatial scales are solar coordinates in arc min where the origin is at the center of the disk (Courtesy of SOHO/UVCS consortium. SOHO is a project of international cooperation between ESA and NASA).

transfer between the fluids, since observations show that the O^{5+} temperature remains higher then the proton and electron temperature, and the protons will not be heated significantly by the O^{5+} due to the small abundance of these ions. In the above equations the Coulomb friction terms $\mathbf{F}_{k,coul}$ can be found in *Braginskii* [1965]. Note, that qualitatively the Coulomb friction increases with the velocity difference between the species, and with the density. The friction decreases when the temperature is increased.

I have used the following normalization: $r \to r/R_\odot$, where $R_\odot$ is the solar radius; $t \to t/\tau_A$; $V \to V/V_A$; $B \to B/B_0$; $n_{i,e,p} \to n_{i,e,p}/n_{e0}$; $S = \tau_r/\tau_A$ the Lundquist number; $\tau_r = 4\pi R_\odot^2/\nu c^2$ the resistive time scale, where ν is the resistivity, and c is the speed of light; $\tau_A = R_\odot/V_A$ the Alfvén time scale; V_A is the single-fluid Alfvén speed; $E_{e,p} = (k_b T_{e,p,0}/m_p)/V_A^2$ the electron or proton Euler number; $E_i = (k_b T_{i,0}/m_i)/V_A^2$ the ion Euler number; $F_r = V_A^2 R_\odot/(GM_\odot)$ the Froude number, where G is the universal gravitational constant and $M_\odot$ is the solar mass; and the normalization constants $a_k = n_{p0}/n_{e0}/A_k + m_e/m_k + A_k n_{i0}/n_{e0}$; $b = cB_0/(4\pi e n_{e0} R_\odot V_A)$, where A_k is the atomic mass of each species, and Z_k is the charge state.

I have used the following parameters in the model: the proton temperature $T_{p0} = 1.6 \times 10^6$ K; the electron temperature $T_{e0} = 1.6 \times 10^6$ K; the O^{5+} temperature $T_{O^{5+}0} = 12 \times 10^6$ K; the electron density $n_{e0} = 10^8$ cm^{-3}; and the O^{5+} density $n_{i0} = 6.2 \times 10^4$ cm^{-3}; the magnetic field $B_0 = 2$ G. These parameters are consistent with recent UVCS observations of streamers [*Kohl et al.*, 1997; *Li et al.*, 1998]. Due to numerical limitations the O^{5+} temperature that I used is larger than the typical O^{5+} temperature ($\sim 5 \times 10^6$) estimated for a coronal streamer. For the above temperatures the proton scale height is $0.14R_\odot$ and the O^{5+} scale height is $0.039R_\odot$. Lower O^{5+} temperature results in smaller ion scale height, and nearly zero O^{5+} density in the core of a streamer that poses a numerical challenge beyond the scope of this study. However, since the Coulomb friction increases for lower O^{5+} temperature the results reported below should hold for $T_{O^{5+}0} = 5 \times 10^6$ K.

To initiate the modeling of the coronal streamer I have used the quadrupole field given by $\mathbf{B} = B_0 r^{-4}[(1-3\cos^2\theta)\mathbf{e}_r - \sin 2\theta \mathbf{e}_\theta]$. The initial proton density and outflow was uniform in θ and given by Parker's[*Parker*, 1963] isothermal solution in r. The initial ion density was taken to be gravitationally stratified (with the gravitational acceleration corrected for the self consistent parallel electric field [*Raymond et al.*, 1997b]), and uniform in θ. The initial uniform density at $r = 1R_\odot$ was chosen to isolate the latitudinal density variations generated by the magnetic configuration above the limb as the simulation evolves to the steady state. The arbitrary initial state is chosen in order to reach the steady state solution in a reasonable computational time. The boundary conditions were imposed at $r = 1R_\odot$, with $V_{k,r} \geq 0$ ($k = p,\ i$), and with incoming characteristics approximated by zero order extrapolation. At $r = r_{max}$, I have allowed for an outflow, and at $\theta = \pi/2, \pi$ I imposed $V_{k,\theta} = B_\theta = 0$, consistent with the quadrupole field geometry. The emphasis of this study is the slow solar wind, therefore, I did not include any additional sources of momentum or heating (such as waves) to produce the fast solar wind.

Numerical Results

I solved the above equations explicitly with the fourth-order Runge-Kutta type method in time, and fourth order

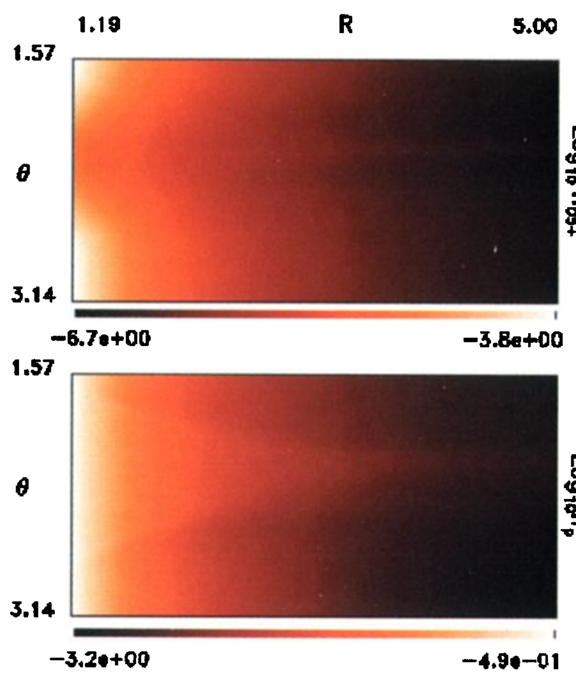

Figure 2. The spatial variations of the O^{5+} (top panel) and proton (bottom panel) densities in the model coronal streamer at $t = 16$ hours.

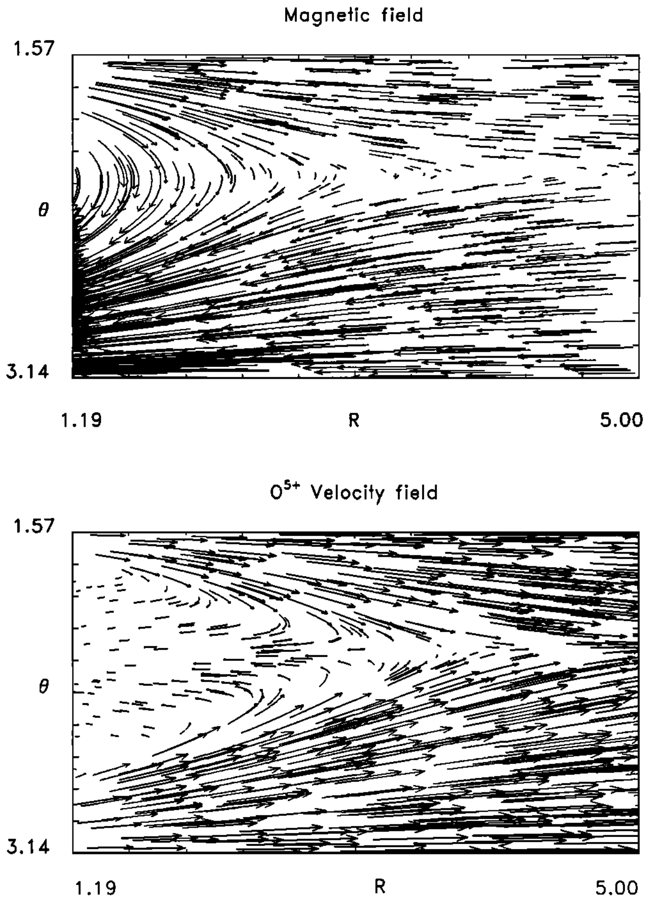

Figure 3. The magnetic field scaled by the square root of the total density (top panel) and the O^{5+} velocity field (bottom panel) of the model coronal streamer at the time shown in Figure 1. The longest velocity vectors correspond to 144 km s^{-1} flows, and the longest magnetic filed vector correspond to 2.6 G.

differencing in space with 160×500 grid cells ($\delta\theta = 0.01$, $\delta r = 0.01$). A fourth order smoothing term was applied for stability. Two-fluid versions of this numerical approach have been used successfully for the modeling of the solar wind flow in coronal holes [*Ofman and Davila*, 1999].

The results of the calculations with the three-fluid code are shown in Figure 2 for the UVCS field of view. The model was run until a streamer with the appropriate sheet current was formed and reached a steady state. The current sheet has a finite thickness and is resolved in the code (the Lundquist number was set to 10^5). The streamer proton density structure and magnetic field structure is in agreement with the single fluid streamer models [*Pneuman, and Kopp*, 1971; *Steinolfson, Suess, and Wu*, 1982; *Washimi, Yoshino, and Ogino*, 1987; *Cuperman, Ofman, and Dryer*, 1990; *Wang et al.*, 1993]. The spatial variations of the proton density n_p, and the O^{5+} density n_i of a model coronal streamer at $t = 16$ hours are shown in Figure 2.

It is evident that the O^{5+} density is enhanced in the open field line regions of the streamer compared to the core, and the proton density is larger in the core of the streamer. The density enhancement at the close field boundary of the streamer is due to the compression by the Lorenz force due to the current sheet, calculated self-consistently in the model (the current sheet and the corresponding density enhancement is below resolution of present coronal observations). The proton density reached a steady state. The qualitative agreement between the model calculations of the proton and ion density structure, and the UVCS observations in Figure 1 is evident. Note, that in Figure 2 I model a streamer belt, while in Figure 1 the streamer is probably more localized in the longitudinal direction. Thus, 3D structure combined with line-of-sight integration of the observed O^{5+} emission of the "hollow" streamer may produce more localized legs.

In the top panel of Figure 3 I show the magnetic field line vectors of the model streamer. The length of the streamline vectors represent the intensity of the magnetic field. The field lines are closed in the core of the streamer. The self consistent streamer field with current sheets results from the time-dependent 2.5D three-fluid calculation. The velocity streamlines are shown in the bottom panel. In the core of the streamer there is small downflow of O^{5+} ions (~ 20 km s^{-1}), and no significant proton flow. Outside the core the flow is along the open field lines. The radial distance of the streamer cusp is determined by the magnetic field strength, geometry, and the plasma pressure (as in the single fluid models).

In the top panel of Figure 4 I show the θ-dependence of the radial velocity of ions (solid lines) and protons (dashed lines) at $1.8R_\odot$ (thick lines) and $5R_\odot$ (thin lines). Outside the streamer core it is evident that the outflow velocity of O^{5+} is close to the outflow velocity of the protons. In the model I find that the outflow velocity is higher in the right leg of the streamer than in the left leg due to the asymmetry of the initial quadrupole field and the corresponding boundary conditions on the field at $r = 1R_\odot$. The magnitude of the outflow speed in the open field regions is in agreement with the outflow velocity for the slow solar wind deduced from UVCS observations using the Doppler dimming effect at this height [*Strachan, et al.*, 2000].

In the bottom panel of Figure 4 I show the θ-dependence of the proton and O^{5+} density. The O^{5+} abundance at the legs shows an order of magnitude enhancement compared to the core, in good agreement with the observations reported by *Raymond et al.* [1997a]. The density spikes at the core

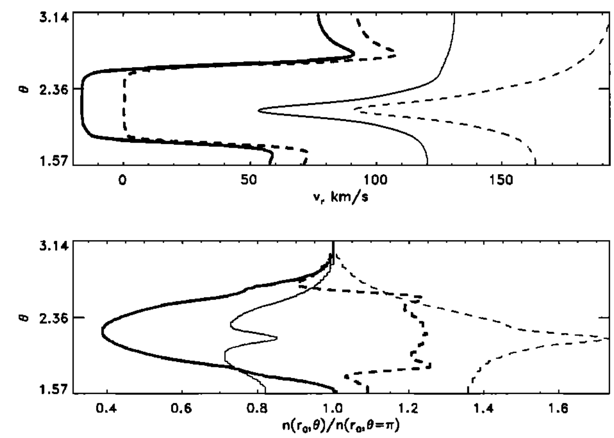

Figure 4. The θ-dependence of the velocity and the density at $r = 1.8R_\odot$ (thick lines) and $r = 5R_\odot$ (thin lines) for the model in Figure 1. The densities are scaled by the values at $\theta = \pi$. Solid lines are for O^{5+}, and the dashed lines are for protons.

boundaries are due to pressure balance with the current-sheet. They are not observed by UVCS, since the thickness of the current sheet is below resolution. The correlation between the outflow velocity, and the O^{5+} density is due to the effect of the Coulomb friction. The main differences in the detail between the model and observations stem from the difference in magnetic topology of the model streamer and the observed coronal streamer, and the possible latitudinal variation of the coronal density and temperature at the coronal boundary.

Conclusions

According to the three-fluid 2.5D MHD numerical model the main mechanism responsible for the observed structure of streamers in O^{5+} is the Coulomb friction between the O^{5+} ions and the outflowing protons. The friction leads to the increase in the density and the outflow speed of the minor ions in the open field regions. The same qualitative enhancement is expected for Fe^{11+} and other minor ions in these regions. In order to verify that the Coulomb friction is the physical mechanism that leads to the enhanced O^{5+} abundance in streamer legs I have repeated the above calculation without the Coulomb friction terms. I found much smaller abundance enhancement of O^{5+} (order of few percent) in the legs of streamers, and an order of magnitude smaller O^{5+} outflow speed in the open field regions. Other possible mechanism that may contribute to the enhanced O^{5+} abundance in the legs of streamers are preferential heating of the ions in these regions, and variations in the ion abundance at the coronal boundary of the legs. These possibilities are left for future studies.

Based on my results, and on recent SOHO/UVCS observations of the solar wind in solar coronal streamers I conclude that the observed enhanced minor ion emission in the legs of streamers is the signature of the slow solar wind outflow regions. The identification of these regions allows to trace the slow solar wind sources low above the limb, and into the extended corona. This will help to understand the origins and the composition of the slow solar wind, and the effect on the interplanetary environment.

Acknowledgments. I would like to thank J.M. Davila, J.C. Raymond, L. Strachan, and A. Van Ballegooijen for fruitful discussions. This work was supported by NASA grant 879-11-38, the NASA SR&T (NASW-98004), and the NASA Space Physics Theory program.

The Editor would like to thank the reviewers of this manuscript.

References

Braginskii, S. I., Transport processes in a plasma, *Rev. Plasma Phys.*, *1*, 205-311, 1965.

Bürgi, A., and Geiss, J., Helium and minor ions in the corona and solar wind - Dynamics and charge states, *Sol. Phys.*, *103*, 347-383, 1986.

Cuperman, S., Ofman, L., Dryer, M., Thermally conductive magnetohydrodynamic flows in helmet-streamer coronal structures, *Astrophys. J.*, *350*, 846-855, 1990.

Esser, R., and Leer, E., Flow of oxygen ions in the solar-wind acceleration region, *J. Geophys. Res.*, *95*, 10269-10272, 1990.

Geiss, J., Hirt, P., and Entwyler, H., On the acceleration and motion of ions in corona and solar wind, *Sol. Phys.*, *12*, 458-483, 1970.

Joselyn, J., and Holzer, T.E., A steady three-fluid coronal expansion for nonspherical geometries, *J. Geophys. Res.*, *83*, 1019-1026, 1978.

Kohl, J.L. et al., First results from the SOHO ultraviolet coronagraph spectrometer, *Sol. Phys.*, *175*, 613-644, 1997.

Li X., Esser, R., Habbal, S.R., Hu, Y.-Q., Influence of heavy ions on the high-speed solar wind, *J. Geophys. Res.*, *102*, 17419-17432, 1997.

Li, J., J. C. Raymond, L. W. Acton, et al., Physical Structure of a Coronal Streamer in the Closed-Field Region as Observed from UVCS/SOHO and SXT/YOHKOH, *Astrophys. J.*, , 506, 431-438, 1998.

Nakada, M.P., A study of the composition of the solar corona and the solar wind, *Sol. Phys.*, *14*, 457-479, 1970.

Noci, G. and et al., The quiescent corona and the slow solar wind, Fifth SOHO Workshop: The Corona and Solar Wind Near Minimum Activity, ESA, *SP-404*, 75-84, 1997.

Pneuman, G.W., and Kopp, R.A., Gas-magnetic field interactions in the solar corona, *Sol. Phys.*, *18*, 258-270, 1971.

Ofman, L., Davila, J.M., Two-fluid 2.5D MHD model of the fast solar wind and the effective proton temperature, Solar Wind Nine, S. Habbal et al. (eds), *AIP Conference Proceedings*, *471*, 405-408, AIP, New York, 1999.

Parker, E.N., Interplanetary Dynamical Processes, New York, Interscience, 1963.

Raymond, J. C., et al., Composition of coronal streamers from the SOHO ultraviolet coronagraph spectrometer, *Sol. Phys.*, *175*, 645-665, 1997.

Raymond, J. C., et al., Absolute abundances in streamers from UVCS, in *Correlated Phenomena at the Sun, in the Heliosphere, and in Geospace*, Proc. 31st ESLAB Symp., ESA publ. SP-415, 383-386, ESA Publications Div., Noodrwijk, The Netherlands, 1997.

Steinolfson, R.S., Wu, S.T., Suess, S.T., The steady global corona, *Astrophys. J.*, *255*, 730-742, 1982.

Strachan, L., et al., Latitudinal dependence of outflow velocities from O VI Doppler dimming observations during the Whole Sun Month, *J. Geophys. Res.*, *105*, 2345-2356, 2000.

Washimi, H., Yoshino, Y., Ogino, T., Two-dimensional structure of the solar wind near the sun, *Geophys. Res. Lett.*, *14*, 487-490, 1987.

Wang, A.-H. et al., A two-dimensional MHD global coronal model - Steady-state streamers, *Sol. Phys.*, *147*, 55-71, 1993.

L. Ofman, NASA GSFC, Code 682, Greenbelt, MD 20771, USA. Leon.Ofman@gsfc.nasa.gov

(Received April 23, 2000; revised June 13, 2000; accepted June 23, 2000.)